Jamming Metal Sheets Using Electropermanent Magnets for Stiffness Modulation

Leah T. Gaeta[1], Vi T. Vo[1], Sang-Yoep Lee[1], Srushti Raste[1], Megha Venkatesam[1], Jacob Rogatinsky[1], M. Deniz Albayrak[1], and Tommaso Ranzani[1,2]

***Abstract*—Soft robots exhibit natural compliance which is desirable in many applications, but often require stiffness modulation techniques when more rigidity is needed. However, many existing stiffening techniques lack portability or fast response times, hindering the ubiquitous adoption of soft robots. Here we introduce a new rapid stiffness modulation method based on magnetism that exhibits portability due to electronic control. This technique jams together thin layers of inherently magnetic metal sheets with a magnetic field generated by electropermanent magnets (EPMs), producing rapid stiffness changes. Quasi-static and dynamic mechanical characterizations for samples with varied layer numbers are presented, highlighting how the magnetic attraction generated by EPMs can be exploited to create a jamming effect. Stiffness increases of up to 68% and energy absorptions of up to 113 mJ were found during quasi-static and dynamic characterizations, respectively. Finally, we demonstrate how this jamming technique can be used in a haptic feedback application and to play a miniaturized version of the game of Skee-Ball®.**

***Index Terms*—Soft Robot Materials and Design, Soft Robot Applications**

I. Introduction

WHILE the inherent compliance of soft robotic devices provides advantages when conforming to and interacting with delicate environments [1], [2], the ability to generate stiffness is often an essential component in soft robot design [3]. Stiffness modulation has been employed in numerous soft robotic applications, such as in surgical robots [4]–[6], graspers [7]–[12], haptics [13], [14], and wearable devices [15]–[19]. Thus, there has been increasing focus on the development of stiffness modulation techniques [3], [20], as these allow soft robotic structures to transition from inherently low stiffness states to more rigid ones, allowing them to transmit force [21]–[27] and reconfigure shape [10], [28], [29].

Jamming-based mechanisms are some of the leading stiffness modulation techniques used in soft robotics [30]. By applying an external stress to a structure composed of packed granular, fibrous, or layered materials, the moment of inertia of the structure increases to generate an instantaneous stiffening effect [30], [31]. Typically the external stresses come in the form of vacuum pressure [22], although positive pressure [15] and magnetism have also recently been employed [24], [32]. Implementation of jamming has been used in a wide variety of soft robotic applications, including wearable devices [13], [33], grasping [7], [8], and shape reconfiguration [28], [29].

Phase change materials have also been investigated as stiffening mechanism in soft robotics. These include shape memory polymers and alloys, which require electronically controlled heating to induce a stiffness change over tens of seconds to minutes [5], [9]. Magnetorheological fluid (MRF) has also been employed as a stiffening mechanism [12], [24]. When a magnetic field is applied to MRF, microscopic iron particles suspended in the fluid immediately align along magnetic field lines to produce a solidification effect [34], and the degree of stiffness can be proportionally tuned with the applied magnetic field [20]. Applications in which phase change materials are implemented to induce stiffness changes include catheters for surgical robots [5], soft gripping [9], and weight-bearing tasks [35].

While these stiffening techniques have been developed for various applications, some drawbacks limit further adoption in soft robotic systems. Despite having fast response times,

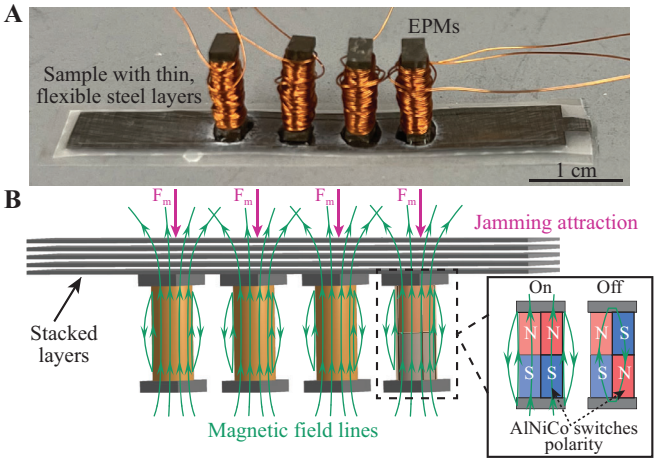

Fig. 1. Jamming of metal sheets with EPMs. A) Sample used during mechanical characterizations. B) Rendering of the jamming principle, showcasing EPMs that are on with magnetic fields displayed (green), magnetically jamming the flexible, thin steel sheets via magnetic attraction forces, F_m (purple). The inset illustrates the working principle of turning an EPM on and off, with the AlNiCo magnet switching polarity.

Manuscript received: January 9, 2025; Revised April 9, 2025; Accepted June 3, 2025.

This paper was recommended for publication by Editor Cosimo Della Santina upon evaluation of the Associate Editor and Reviewers' comments. This work was supported by the Office of Naval Research (ONR) grant number N00014-22-1-2244. The content is solely the responsibility of the authors and does not necessarily represent the official views of the ONR. The work of V.T. Vo was supported by NSF Graduate Research Fellowship under Grant 2234657.

[1]L.T. Gaeta, V.T. Vo, S.-Y. Lee, S. Raste, M. Venkatesam, J. Rogatinsky, M.D. Albayrak, and T. Ranzani are with the Department of Mechanical Engineering, Boston University, Boston, MA 02215 USA.

[2]T. Ranzani is with the Department of Biomedical Engineering and Materials Science and Engineering Division, Boston University, Boston, MA 02215, USA tranzani@bu.edu

Digital Object Identifier (DOI): see top of this page.

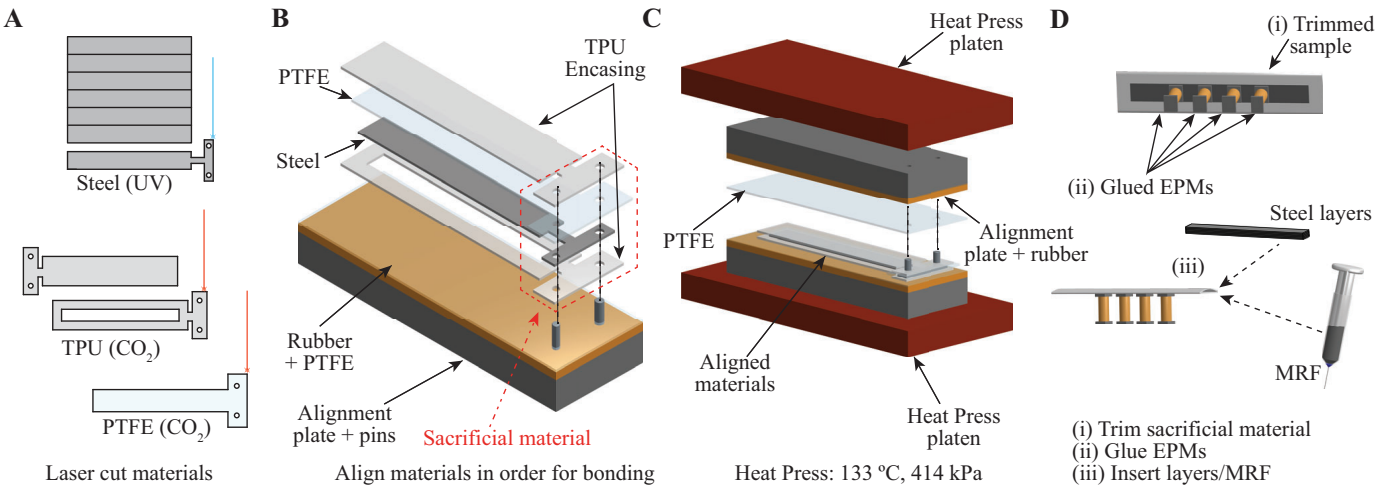

Fig. 2. Overview of the fabrication process for a sample subjected to magnetic jamming using EPMs. A) Materials are cut to size using UV and CO_2 lasers. B) Layers of TPU, steel, and PTFE are aligned. C) Aligned materials are selectively bonded via a heat press for two minutes. D) Four EPMs are glued to the exposed steel layer, and additional steel layers and MRF are added to the sample as needed, then sealed.

the external pneumatic pressure sources required for jamming often limit portability as the pumps can add bulk and noise. Meanwhile, phase change materials provide the benefit of electronic control and thus portability in many soft robotic applications, but the response time for inducing a stiffness change is slow (tens of seconds to minutes) [5], [9].

In this paper, we focus on electronically inducing magnetic fields to jam stacks of flexible steel sheets using electropermanent magnets, or EPMs. EPMs have previously been used in soft robotic actuators [36], valves [37], and wearable devices [17], as they provide the advantage of being able to switch magnetic fields on and off like electromagnets, but without continuous power consumption; that is, only in the act of switching between on/off states over microseconds is power consumed [38]. We stack five, ten, fifteen, and twenty layers of thin (25 μm thick), compliant, and inherently magnetic metal sheets, and study how electronically applied magnetic fields can be used to instantaneously jam these sheets, both with and without MRF. Previous work from our group has introduced magnetically induced stiffening, which combines the mechanical elements of jamming, such as granules, fibers, and layers, with MRF [24]. While this technique demonstrates magnetic-based jamming, permanent magnets and MRF were required for stiffness modulation. In this work, however, EPMs are implemented and the addition of MRF is not required due to the magnetic nature of the layered steel sheets, as depicted in Figure 1, though MRF can be used as a design tool to further tune stiffening performance. In addition to designing metal-based jamming beams, we also provide quasi-static and dynamic behavior analyses that showcase achievable stiffening ranges and damping capacity, respectively. Previous work on magnetically induced stiffening only highlighted quasi-static mechanical characterizations; thus, the dynamic behavior analysis provided here emphasizes how our jamming technique can be exploited as a damping element for robotic systems. The stiffening effects that are induced via this magnetic jamming method are demonstrated in a wearable haptic device for robot to human communication, to showcase the quasi-static behavior, and in playing a game similar to Skee-Ball®, which highlights the dynamic behavior.

This form of magnetic jamming provides the advantages of electronic control for portability by removing the need for bulky pumps seen in pressure-based jamming, nearly instantaneous timing, and tunable stiffness ranges. Further, we demonstrate how this new technique can be used in a wide range of applications and inform soft robot design.

II. Design & Manufacturing

A. Magnetic Jamming Samples

To study the effects of magnetically jamming metal sheets, samples with various combinations of steel sheets and MRF were fabricated. Low-carbon steel sheets of 25μm thickness (McMaster-Carr) were sanded with 220 grit sandpaper on both sides to increase friction between layers, then cut into 42 mm $\times$ 6 mm layers using a UV laser (Coherent, Matrix-355), as depicted in Fig. 2A. By increasing the friction between layers, the samples can act more like a single cohesive beam unit when magnetically jammed, thereby also increasing bending stiffness [22], [24], [30]. Thermoplastic polyurethane of 38μm thickness, or TPU (American Polyfilm), and 25μm thick polytetrafluoroethylene, or PTFE (Teflon, McMaster-Carr), layers were then cut using a CO_2 laser (VersaLaser, VLS6.60) into rectangular pieces of 46 mm $\times$ 10 mm and 43.5 mm $\times$ 7.5 mm, respectively (Fig. 2A). For each fabricated sample, one TPU layer had a 40 mm $\times$ 4 mm window cut out to expose a steel layer that was later used as the surface for gluing EPMs (Fig. 2D). To form a single sample encasing, the layers are aligned in the following order: TPU layer with window, steel layer, PTFE layer, and TPU layer without a window (Fig. 2B). The PTFE layer between the steel and final TPU layer acted as a mask to ensure that the steel did not stick to this final TPU layer. Note that the layers have additional sacrificial material solely used for material alignment with dowel pins, as seen in Fig 2A-C. The aligned layers were

then heat pressed (Carver, 5420) for two minutes at 133 °C and 414 kPa (Fig. 2C). After heat pressing, the sacrificial material used for alignment was trimmed and the PTFE layer was removed to reveal a 46 mm × 10 mm encasing with an opening (Fig. 2D). Four EPMs were then glued (Loctite, 4861) via their endcaps to the exposed steel window, each of them symmetrically placed 6 mm apart from endcap centers. This 6 mm distance was determined based upon previous work that analyzed how the magnetic field changed with distance away from an EPM [17]. Placing the EPMs 6 mm apart ensured that they would not interact with other while still imparting a jamming effect. Steel layers were then inserted into the opening of fabricated encasings to form samples of five, ten, fifteen, and twenty layers (these layer samples include the initial single steel layer used during alignment and heat bonding). Steel layers and 0.01 mL of MRF (MRF-140CG, Lord) were also inserted to form four additional samples of five, ten, fifteen, and twenty layers with the added MRF. The eight total samples were then hand-sealed (Spot-Crimp Hand-Held Heat Sealer, McMaster-Carr) to hold the materials inside.

B. Electropermanent Magnets

To demonstrate the magnetic stiffening of stacked thin steel layers, EPMs are used, as seen in Fig. 1. Our EPMs are an assembly of two cylindrical magnets that are axially magnetized (1.6 mm in diameter and 6.35 mm long) and adhered side-by-side between two 3.6 mm × 2 mm A36 low-carbon steel endcaps of 0.8 mm thickness (McMaster-Carr). The two magnets have similar remanent flux, but different coercivities: a soft AlNiCo 5 magnet (Eneflux Armtek Magnetics) of low coercivity and a hard NdFeB N42 magnet (K&J Magnetics) with high coercivity. These magnets are wrapped with 36AWG copper wire (McMaster-Carr) for 75 turns. Given that magnetic fields can be increased by decreasing endcap thickness [38], the endcap thickness of 0.8 mm led to increased generated magnetic fields compared to previous designs [17], [36], [37] while still maintaining structural integrity of an EPM. A thinner endcap could possibly cause magnetic flux to circulate through the layers and thus a thickness of 0.8 mm ensures the EPMs can switch between on and off states to jam and unjam samples.

When a short pulse of current is applied to one end of the copper coil around the EPM, the polarity of the soft AlNiCo magnet reverses and turns on the EPM. When current is applied to the other end of the coil, polarity of the soft AlNiCo flips back and turns the EPM off. When switching EPM states, we apply 20 V for 500 μs, which consumes 50 mJ of nearly instantaneous energy (this energy value is calculated following equations from previously published works [37], [38]). This was done for all of the EPMs throughout the experiments and demonstrations presented in this paper. Magnetization and demagnetization of the EPMs was achieved using a microcontroller (Arduino Nano) and four pairs of BTN8962TA half-bridge integrated circuits (Infineon Technologies) on a customized printed circuit board (JLCPCB), with a benchtop power supply (B&K Precision 1671A) to produce the 20 V required for each EPM. Using a gaussmeter to measure magnetic field (LakeShore Cryotronics, 425), each EPM exhibits 45 mT and 0 mT at the endcaps when on and off, respectively. Because the magnetic field is strongest at the endcaps of an EPM, the EPMs are adhered to the samples in the vertical arrangement presented in Figure 1, since a horizontal arrangement would produce weaker magnetic attraction [17]. When in the on state, the magnetic attraction force of an EPM on a stack of steel layers, F_M, was measured to be 95.67 mN (see supplementary video).

III. Methods and Results

A. Quasi-Static Mechanical Characterization

The quasi-static behavior of the fabricated beams was tested in three point bending, as pictured in Fig. 3A. Roller supports and an anvil with radii of 2.5 mm were designed, 3D-printed (Bambu Lab), and affixed to a tensile testing machine (Instron, 5943). The anvil was attached to a 50 N load cell with 100 mN resolution, and lowered at a rate of 10 mm/min over the center of each sample, which would sit atop roller supports that were separated by 30 mm. A 5 mm displacement was imposed on all samples under two conditions: (1) with no EPMs on and thus no magnetic field applied, and (2) with magnetic field applied by turning all EPMs on. The data that was collected is presented in Fig. 3 and tabulated in Table I.

The stiffness (K), which is taken from a linear fit of the slopes of the force vs. displacement curves, increased for each sample once a magnetic field was supplied by the EPMs. In addition, the initial stiffness (K_0) of the samples without magnetic field applied increased with increasing layer number (i.e. a twenty layer sample was stiffer than a five layer sample). Further, the addition of MRF also increased the initial stiffness of the samples compared to those with the same number of layers but no MRF.

TABLE I
Results of the quasi-static mechanical characterization

Sample	K_0 [mN/mm]	K [mN/mm]	K/K_0
5 Layers	16.66	23.67	1.42
10 Layers	28.41	47.76	1.68
15 Layers	46.56	61.25	1.32
20 Layers	56.04	64.76	1.16
5 Layers + MRF	19.36	26.84	1.39
10 Layers + MRF	37.85	49.61	1.31
15 Layers + MRF	51.50	64.63	1.25
20 Layers + MRF	67.93	85.16	1.25

While the stiffness of all samples without MRF increased when magnetized, the 10 Layer sample experienced the largest increase and the 5 Layer sample the next largest increase, as observed when normalizing by each sample's initial stiffness, K_0 (see Table I). The stiffness, K, of the 10 Layer and 5 Layer samples when magnetized increased by 68% and 42%, respectively, while the increases for the 15 and 20 Layer samples were only 32% and 16%, respectively. This suggests that the EPMs used in this experiment produce a greater stiffening effect when there are ten or fewer layers, likely because the strength of magnetic attraction decreases the further a layer is from the EPMs, thus lessening the jamming

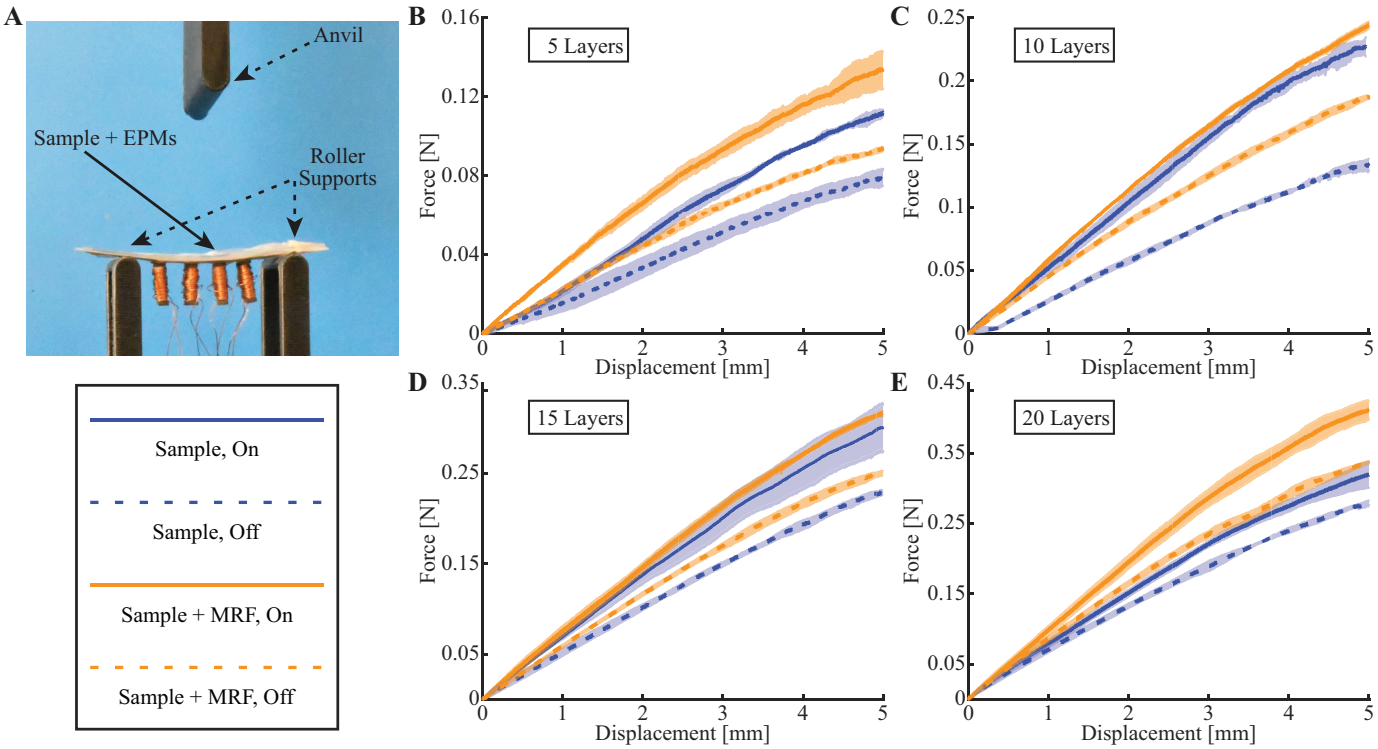

Fig. 3. Quasi-static force vs. deflection results from magnetically jamming metal sheets. A) Experimental setup for quasi-static characterization. Experimental results from when EPMs were turned on (solid curves) and turned off (dashed curves) are displayed for 5 layers and 5 layers with MRF in (B), 10 layers and 10 layers with MRF in (C), 15 layers and 15 layers with MRF in (D), and 20 layers and 20 layers with MRF in (E). Each curve displays the mean of three trials with the shaded error bar representing one standard deviation.

effect on thicker stacks. This is also supported by the samples that also contain MRF. Both the 5 Layer and 10 Layer samples that had additional MRF experienced greater increases in stiffening, 39% and 31% respectively, than the 15 and 20 Layer samples with MRF, which both increased by 25%. However, the addition of MRF appears to improve the jamming effect for the 20 Layer samples, possibly because the suspending iron particles are coating the layers and thus help strengthen the attraction of the farther layers towards the EPMs. Thus, MRF is not needed for samples of 15 layers or less, unless required for design reasons. Also of note is the lack of slip point observed. Three-point bending analysis of vacuum-based layer jamming yields a distinct slip point in which shear forces induced within a jammed structure overcome coupling frictional forces between layers [22], [26], [30]. By using magnetism to jam layers, the EPMs impose attractive forces that cause the layers to stick as if one cohesive beam unit and any shear forces resulting from an imposed displacement are likely too small to measure, leading to an unobservable slip point.

Compared to previously reported jamming methods, the stiffening range resulting from this jamming technique is also narrower. For instance, in pressure-based layer jamming stiffness increases of 1800:1 are reported [27], and in other magnetically induced stiffening methods increases of 344% are observed [24]. The observed reduced stiffness ratio is likely due to a number of factors. While the added mass of EPMs impacts stiffening ranges, the magnitude of the magnetic fields generated and the discrete jamming nature of this method likely yield smaller stiffness ratios compared to other layer jamming techniques. However, pressure-based layer jamming requires pneumatic components which add bulk and limit portability, and previous magnetic stiffening methods for layer jamming required MRF and strong NdFeB permanent magnets exhibiting magnetic fields of up to 436 mT. This particular magnetic jamming technique, in contrast, is more portable than pneumatic layer jamming due to the removal of additional equipment, can work with electronically driven magnetic fields that are smaller, and does not require MRF.

B. Dynamic Mechanical Characterization

Dynamic characterization was performed on samples with varying numbers of layers to investigate the dynamic responses, including both transient and steady-state behaviors when subjected to an initial displacement. This analysis is important for evaluating the effectiveness of our jamming method in tuning mechanical impedance, or the stiffness and damping, of a system. The ability to dynamically adjust these mechanical properties in response to external forces can enhance the adaptability of soft robotic systems and devices.

While the quasi-static behavior of beams subjected to the magnetic jamming was evaluated using three point bending, the dynamic behavior of the beams was analyzed in cantilever bending. Each sample was fixed at one end using a customized, 3D-printed fixture (Bambu Lab), while a fiducial marker was placed at the other end, which was free to move, as depicted

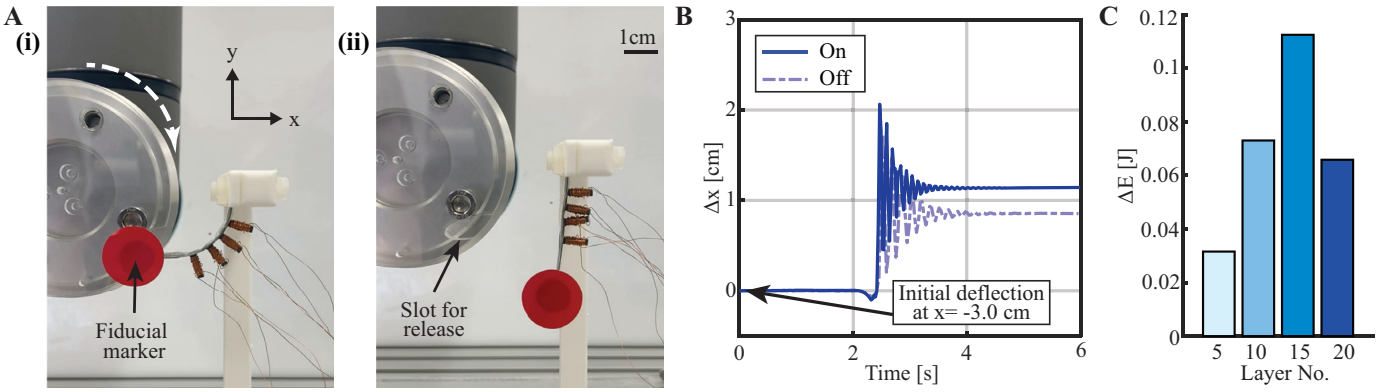

Fig. 4. Characterization of the dynamic responses from magnetically jammed stacked metal sheets. A) Experimental setup for dynamic characterization. B) A sample of the step response with 5 Layers at an initial deflection of x = -3 cm. C) Increase in energy of the samples observed from the step responses following the release of a sample when magnetized by the EPMs.

in Fig. 4A. At the start of a test, the free end was held by a customized acrylic fixture that was attached to a robot arm (Universal Robots), which initially displaced the free end 3.0 cm away in the negative x-direction (Fig. 4A). The robot arm was then programmed to release the free end by rotating the attached acrylic piece, and the cantilevered beam would oscillate until it settled to a steady-state position at the rest. A camera (iPhone 13) was used to capture the movement of the fiducial marker at 60 frames per second as each sample was tested in both unmagnetized and magnetized states (three trials were conducted for each sample in both states). We then captured the response of the beam by tracking the movement of the fiducial markers. This process involved converting the centroid position of the marker from pixel coordinates to real-world units based on a scale factor, which was calculated by comparing the pixel area of the circular marker to its known physical area. Time-series data for the marker positions were generated by associating the frame indices with the video frame rate. Image processing and visualization were performed using custom MATLAB scripts (version R2024a, MathWorks Inc.) with the Image Processing Toolbox. The dynamic responses of the beams with different numbers of layers and magnetization are illustrated in Fig. 4B, which depicts the results for the 5 Layer sample. Note that since the quasi-static mechanical characterization for the samples with MRF did not generate as dramatic of changes in stiffness when magnetized, only samples that did not have MRF were subjected to dynamic behavior characterization. Further, we observed that when the samples with MRF were initially deflected when magnetized, the beams would retain the initially curved state, suggesting that magnetized MRF can be useful for shape-locking and shape-reversibility purposes. We hypothesize that under dynamic conditions, such as rapid oscillatory motion, the fluid's magnetized rheological property may increase viscous damping, leading to increased energy dissipation, and the viscoelasticity of the fluid results in non-linear mechanical responses. As we are using a linear model, characterizing the behavior of the samples with MRF may not be appropriate.

In order to further evaluate how magnetic jamming with EPMs affects the dynamic properties, we performed 1) parameter identification for a lumped second-order dynamics equation and 2) frequency-domain analysis with Fourier transform on the achieved time-series position datasets.

First, the time-displacement responses were modeled using second-order dynamic equations. The effect of magnetic jamming on the dynamic properties was examined by representing the system as an equivalent mass-spring-damper model. The motion following the release of the system was free vibration, and the corresponding equation can be written as:

$$m\ddot{x} + c\dot{x} + kx = 0. \tag{1}$$

Since beams with the same number of layers share the same inertial configuration, magnetized or not, the mass-specific damping and spring coefficients were derived due to redundancy in Equation (1).

$$\ddot{x} + c^*\dot{x} + k^*x = 0 \tag{2}$$

where $c^* = c/m$ and $k^* = k/m$.

The constant parameters c^* and k^* were then determined using the least squares method:

$$c^*,\ k^* = \underset{c^*,\ k^*}{\arg\min} \sum_t (\ddot{x} + c^*\dot{x} + k^*x)^2 \tag{3}$$

The identified parameters are summarized in Table II. In all cases, engaging the magnetization increased both the damping and stiffness, with a larger proportional increase observed in stiffness.

In addition, we conducted a frequency domain analysis on the time-series data to evaluate system responses across various frequencies, isolating the changes in stiffness and damping that influence a system's energy (or resistance to external forces). In some cases, the peak in the frequency domain was not clearly identifiable because the motion following the release did not persist long enough. Instead, the change in overall energy (ΔE) of the motion was calculated by subtracting the integrals of the squared frequency responses when the EPMs were magnetized (X_{ON}) and demagnetized (X_{OFF}) over the frequency range (in Hz):

$$\Delta E = \int |X_{ON}(f)|^2 df - \int |X_{OFF}(f)|^2 df \tag{4}$$

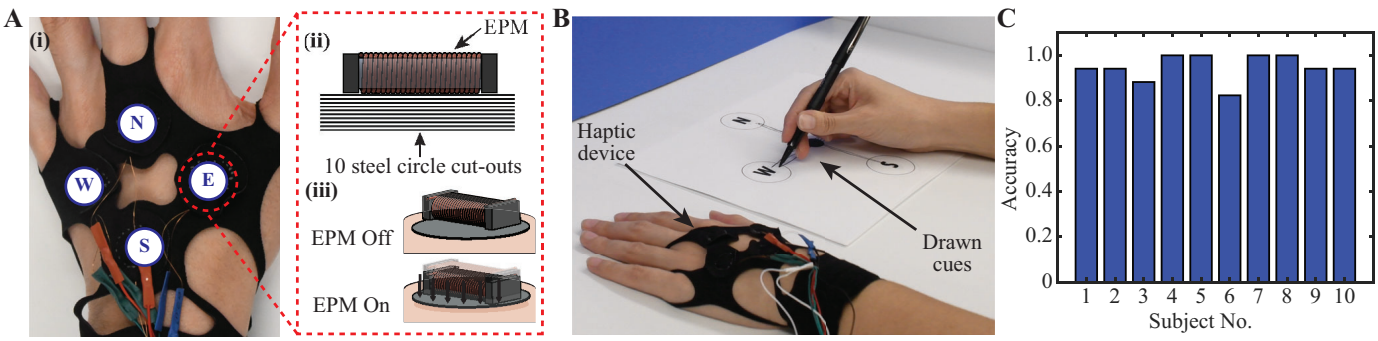

Fig. 5. Demonstration of instantaneous stiffening by jamming metal sheets using EPMs in a haptic communication application. A) The device is worn on the hand's dorsal surface with north (N), south (S), east (E), and west (W) locations labeled (i). An EPM lies atop a stack of ten circular steel sheets (ii) and provides the haptic cue by briefly turning on then off (iii). B) Participant receives haptic cues on their non-dominant hand and draws a line with the dominant hand in the direction of the perceived cue. C) Accuracy results obtained from ten participants.

TABLE II
RESULTS OF THE DYNAMIC MECHANICAL CHARACTERIZATION

Layer No.	Magnetization	c^* [Ns/kgm]	k^* [N/kgm]
5 Layers	OFF	4.35	1476.47
	ON	4.85	1747.94
10 Layers	OFF	8.48	2609.87
	ON	14.39	2806.64
15 Layers	OFF	14.64	2940.54
	ON	23.34	3535.28
20 Layers	OFF	14.53	3364.33
	ON	25.51	3791.04

where $x(t) \xrightarrow{\mathcal{F}} X(f)$ and $\mathcal{F}$ denotes the Fourier transform $X(f) = \int x(t)e^{-j2\pi ft}dt$.

The calculated energy increased across all samples when magnetized: by 31.6 mJ for 5 layers, 73.0 mJ for 10 layers, 112.5 mJ for 15 layers, and 65.8 mJ for 20 layers, as illustrated in Fig.4C. These energy increases are not to be confused with the 50 mJ required to change EPM states, as previously mentioned in Section II-B.

For the same structural configuration, the oscillations following the release became larger and faster after magnetization. Magnetization significantly increases k^* as shown in Table II, increasing the natural frequency ($\omega = \sqrt{k^*}$) and thus, resulting in faster oscillations. For example, for 15 layers, c^* increases by 59.42% and k^* increases by 20.23%. Although c^* also increases with magnetization, its relative growth is smaller than that of k^*, resulting in reduced damping ratios ($\zeta = c^*/2\sqrt{k^*}$), allowing for larger oscillation amplitudes. Similarly, increasing the number of layers further increases k^*, resulting in faster oscillations. For instance, with the EPMs magnetized c^* increases by 426.0% and k^* increases by 116.9% from 5 to 20 layers. Notably, the 15-layer sample exhibited the largest increase, attributed to the optimal balance between the structural rigidity provided by additional layers and the jamming effect induced by the magnetization of the EPMs.

The results demonstrate that magnetizing the EPMs and increasing layer numbers both contribute to a higher equivalent stiffness and damping, normalized with respect to sample mass, thereby amplifying the speed and size of the oscillations. Thus, stiffer configurations enable a system to become more resistant to deformation as it absorbs more energy under dynamic conditions, making it more suitable for applications involving impact mitigation or contact with the environment. By demonstrating these two outcomes from the analytical processes, we have verified that this magnetic stiffening technique can be utilized to enhance variable dynamic properties in the soft robot design process.

C. Demonstration of Haptic-Based Communication

To demonstrate the quasi-static behavior of magnetic jamming with EPMs, the stiffening technique was implemented in a soft robotic haptic device. The device was fabricated using a 1.5 mm thick neoprene textile (SewSwank) that was designed to sit over the dorsal surface of the hand, as depicted in Fig. 5A. With loops laser cut for the thumb, middle, and little fingers and an adjustable Velcro wrist strap, the device can reasonably fit over a range of hand sizes. On the exterior surface of this textile, four pouches were sewn in a design intended to mimic the north, south, east, and west directions of a compass (see Fig. 5A-i). Informed by the experimental characterization presented in Section III-A, one EPM that sat atop ten layers of steel circles of 1 cm in diameter was inserted into each of the four pouches (Fig. 5A-ii). Note that to help minimize device form factor, the EPMs were placed on the layers horizontally, rather than vertically (as was used in the mechanical characterization). The wires for the EPMs were then connected to the same PCB used in the previously described experiments.

The device was then worn on a participant's nondominant hand while the dominant hand was used to draw in the direction of a given cue. For example, with the EPMs set to 20 V via a benchtop power supply (B&K Precision 1671A) the researcher would send a command using a microcontroller (Arduino Nano) to one of four directions. The command for each direction was composed of a 500 μs pulse to turn the EPM on, followed by a 500 μs pause, and ending with a 500 μs pulse to turn the EPM back off. The instantaneous stiffening effect induced by the jamming of metal sheets provided a

momentary mechanical force that would be interpreted by the participant as a haptic cue (Fig. 5A-iii). After a brief training period for the participant, the researcher would input a randomized sequence of 17 directional cues (e.g. EWNSS-WNEEWNESSWNE), that the participant was blind to, and the participant would use their dominant hand to draw from the center of an enlarged printed compass towards the cue that the participant perceived (see Fig. 5B). The participant would then return the pen to the center, indicating to the researcher to send the next cue.

In all, ten participants were recruited to demonstrate the device. Four participants interpreted the haptic cues with 100% accuracy while one participant had the lowest score of 82% accuracy. The mean accuracy among all ten participants was 94.7% and the results are displayed in Fig. 5C.

D. Demonstration of Metal Jamming Dynamics

We also applied the dynamic behavior of a sample subjected to the magnetic jamming stiffening effect to play a miniaturized and modified game of Skee-Ball®. Using the same apparatus implemented during the dynamic mechanical characterization described in Section III-B, a 10 Layer sample was cantilevered and used to hit a 7 mm in diameter ball up the ramp of a customized game fixture. Both the ramp and the ball were 3D-printed (Bambu Lab), and the 10 Layer sample was used to try and score the ball through one of the four holes. Players would use a finger to pull the free end of the beam back behind the ball and then release, striking the ball and causing it to travel up the ramp to either score through one of the holes for points, hit the backboard and drop for zero points, or return back to the start. The game is depicted in Figure 6 and players would attempt to score over two turns; one with the EPMs turned off and one with the EPMs all on, applying the magnetic field necessary to jam the ten steel layers together and stiffen the beam. Among all players, it was difficult to score a point when the EPMs were off (20 % success) as the ball often lacked the energy required to travel all of the way up the ramp. However, the ball would often score a point on the second turn when all of the EPMs were turned on to stiffen the beam before striking the ball (90% success).

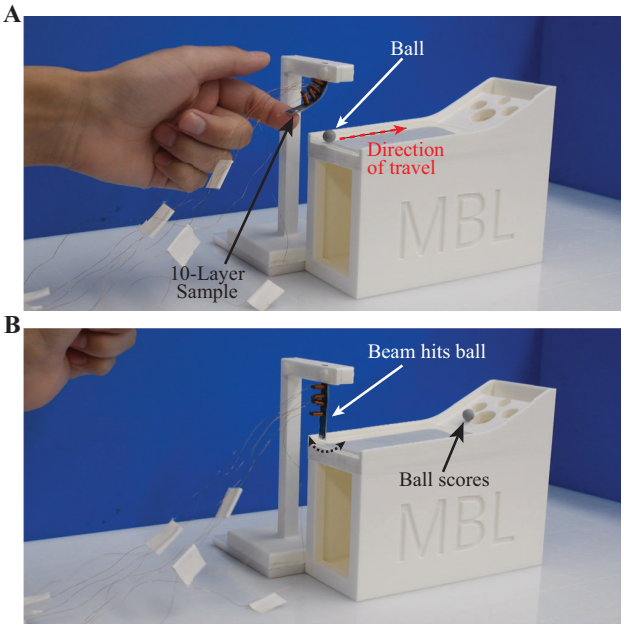

Fig. 6. Demonstration of the dynamic behavior of a beam jammed by EPMS used to play a modified game of Skee-Ball®. A) The beam is pulled back before releasing. B) The released beam strikes the ball, which travels up the ramp and scores points by falling through one of the holes.

IV. Conclusion

In this paper, we highlight how jamming stacks of metal sheets with EPMs can be an effective stiffness modulation technique for soft robotics. By stacking five to twenty layers of very thin steel and applying a magnetic field using EPMs, the layers jam together to increase the overall stiffness. The primary benefit of this stiffening technique is the application of magnetic field. Due to the inherent magnetic attraction of the steel layers to the EPMs, the layers immediately jam once magnetism is induced, thus providing an instantaneous stiffening effect. The advantageous properties of EPMs also allow for the stiffening effect to be imposed without continuously consuming power, like an electromagnet. The EPMs only consume power when changing states, which is on the order of microseconds and thus only require 50 mJ of energy to do so. Further, EPMs are electronically controlled, which is often a desirable feature for soft robotic devices that require portability. In contrast to other stiffening mechanisms, such as phase change materials which boast electronic control but slower response times, or traditional jamming which provide rapid response times but limit portability due to the required pneumatic components, this form of magnetic jamming combines the best features of these techniques: electronic control and immediate response times. Previous research on magnetic stiffening also relied on permanent magnets, limiting usability in robotic systems, and the former requirement of MRF is no longer needed, thereby lowering cost, improving overall profile, and reducing fabrication time for a robotic system requiring magnetic stiffening. Thus, this work can open the door towards developing future soft robotic designs in applications that require stiffness modulation.

Besides presenting the fabrication methods for both the metal beams and the EPMs, we also mechanically characterized the quasi-static and dynamic behavior of the beams when magnetically jammed and unjammed. The stiffening technique was also used to demonstrate its applicability in a wearable haptic feedback device that provides directional cues in which the mean accuracy among ten users was ≈95%, and in playing a version of a classic arcade game where stiffened beams resulted in a 90% success rate for scoring points (compared to 20% with unstiffened beams). In future work, we aim to expand further on the customizability prospects for this stiffening technique. This can be accomplished by studying various on/off state combinations of the EPMs, as well as by modifying the pulse durations sent to each EPM and how these affect the strength of the magnetic field at the end caps. Studying the jamming behavior of magnetic fibers and

granules would also be valuable as this would be analogous to current fiber and granular pressure-based jamming techniques in the state of the art.

REFERENCES

[1] B. Jumet, M. D. Bell, V. Sanchez, and D. J. Preston, "A Data-Driven Review of Soft Robotics," *Advanced Intelligent Systems*, vol. 4, no. 4, p. 2100163, 4 2022.

[2] C. Laschi, B. Mazzolai, and M. Cianchetti, "Soft robotics: Technologies and systems pushing the boundaries of robot abilities," *Science Robotics*, vol. 1, no. 1, 2016.

[3] M. Manti, V. Cacucciolo, and M. Cianchetti, "Stiffening in soft robotics: A review of the state of the art," *IEEE Robotics and Automation Magazine*, vol. 23, no. 3, pp. 93–106, 9 2016.

[4] T. Ranzani, M. Cianchetti, G. Gerboni, I. D. Falco, and A. Menciassi, "A Soft Modular Manipulator for Minimally Invasive Surgery: Design and Characterization of a Single Module," *IEEE Transactions on Robotics*, vol. 32, no. 1, pp. 187–200, 2 2016.

[5] J. Lussi, M. Mattmann, S. Sevim, F. Grigis, C. De Marco, C. Chautems, S. Pané, J. Puigmartí-Luis, Q. Boehler, and B. J. Nelson, "A Submillimeter Continuous Variable Stiffness Catheter for Compliance Control," *Advanced Science*, vol. 8, no. 18, 9 2021.

[6] P. Lloyd, T. L. Thomas, V. K. Venkiteswaran, G. Pittiglio, J. H. Chandler, P. Valdastri, and S. Misra, "A Magnetically-Actuated Coiling Soft Robot With Variable Stiffness," *IEEE Robotics and Automation Letters*, 6 2023.

[7] Y. Li, Y. Chen, Y. Yang, and Y. Wei, "Passive Particle Jamming and Its Stiffening of Soft Robotic Grippers," *IEEE Transactions on Robotics*, vol. 33, no. 2, pp. 446–455, 4 2017.

[8] E. Brown, N. Rodenberg, J. Amend, A. Mozeika, E. Steltz, M. R. Zakin, H. Lipson, and H. M. Jaeger, "Universal robotic gripper based on the jamming of granular material," *Proceedings of the National Academy of Sciences*, vol. 107, no. 44, pp. 18 809–18 814, 2010.

[9] R. Coulson, C. J. Stabile, K. T. Turner, and C. Majidi, "Versatile Soft Robot Gripper Enabled by Stiffness and Adhesion Tuning via Thermoplastic Composite," *Soft Robotics*, vol. 9, no. 2, pp. 189–200, 4 2022.

[10] E. J. Barron III, E. T. Williams, R. Tutika, N. Lazarus, and M. D. Bartlett, "A unified understanding of magnetorheological elastomers for rapid and extreme stiffness tuning," *RSC Applied Polymers*, vol. 1, no. 2, pp. 315–324, 2023.

[11] Y. Yang, K. Vella, and D. P. Holmes, "Grasping with kirigami shells," *Science Robotics*, vol. 6, no. 54, p. 6426, 5 2021.

[12] A. Pagoli, M. Alkhatib, and Y. Mezouar, "A Soft Variable Stiffness Gripper with Magnetorheological Fluids for Robust and Reliable Grasping," *IEEE Robotics and Automation Letters*, vol. 9, no. 5, pp. 4519–4526, 5 2024.

[13] S. Jadhav, M. R. A. Majit, B. Shih, J. P. Schulze, and M. T. Tolley, "Variable Stiffness Devices Using Fiber Jamming for Application in Soft Robotics and Wearable Haptics," *Soft Robotics*, vol. 9, no. 1, pp. 173–186, 2 2022.

[14] A. A. Stanley and A. M. Okamura, "Controllable Surface Haptics via Particle Jamming and Pneumatics," *IEEE Transactions on Haptics*, vol. 8, no. 1, pp. 20–30, 1 2015.

[15] T. Liu, H. Xia, D. Y. Lee, A. Firouzeh, Y. L. Park, and K. J. Cho, "A positive pressure jamming based variable stiffness structure and its application on wearable robots," *IEEE Robotics and Automation Letters*, vol. 6, no. 4, pp. 8078–8085, 10 2021.

[16] T. P. Chenal, J. C. Case, J. Paik, and R. K. Kramer, "Variable Stiffness Fabrics with Embedded Shape Memory Materials for Wearable Applications," in *IEEE/RSJ International Conference on Intelligent Robots and Systems (IROS)*. IEEE, 2014, pp. 2827–2831.

[17] L. T. Gaeta, M. D. Albayrak, L. Kinnicutt, S. Aufrichtig, P. Sultania, H. Schlegel, T. D. Ellis, and T. Ranzani, "A magnetically controlled soft robotic glove for hand rehabilitation," *Device*, p. 100512, 8 2024.

[18] A. T. Wanasinghe, W. V. Awantha, A. G. Kavindya, A. L. Kulasekera, D. S. Chathuranga, and B. Senanayake, "A Layer Jamming Soft Glove for Hand Tremor Suppression," *IEEE Transactions on Neural Systems and Rehabilitation Engineering*, vol. 29, pp. 2684–2694, 2021.

[19] V. Sanchez, C. J. Walsh, and R. J. Wood, "Textile Technology for Soft Robotic and Autonomous Garments," *Advanced Functional Materials*, vol. 31, no. 6, 2 2021.

[20] Y. Yang, Y. Li, and Y. Chen, "Principles and methods for stiffness modulation in soft robot design and development," *Bio-Design and Manufacturing*, vol. 1, no. 1, pp. 14–25, 3 2018.

[21] J. Choi, D. Y. Lee, J. H. Eo, Y. J. Park, and K. J. Cho, "Tendon-driven jamming mechanism for configurable variable stiffness," *Soft Robotics*, vol. 8, no. 1, pp. 109–118, 2 2021.

[22] Y. S. Narang, J. J. Vlassak, and R. D. Howe, "Mechanically Versatile Soft Machines through Laminar Jamming," *Advanced Functional Materials*, vol. 28, no. 17, 4 2018.

[23] R. Baines, B. Yang, L. A. Ramirez, and R. Kramer-Bottiglio, "Kirigami layer jamming," *Extreme Mechanics Letters*, vol. 64, 11 2023.

[24] L. T. Gaeta, K. McDonald, L. Kinnicutt, M. Le, S. Wilkinson-Flicker, Y. Jiang, T. Atakuru, E. Samur, and T. Ranzani, "Magnetically Induced Stiffening for Soft Robotics," *Soft Matter*, 2023.

[25] D. Bruder, M. A. Graule, C. B. Teeple, and R. J. Wood, "Increasing the payload capacity of soft robot arms by localized stiffening," *Science Robotics*, vol. 8, no. 81, 8 2023.

[26] Y. S. Narang, A. Degirmenci, J. J. Vlassak, and R. D. Howe, "Transforming the dynamic response of robotic structures and systems through laminar jamming," *IEEE Robotics and Automation Letters*, vol. 3, no. 2, pp. 688–695, 4 2018.

[27] Y. S. Narang, B. Aktas, S. Ornellas, J. J. Vlassak, and R. D. Howe, "Lightweight Highly Tunable Jamming-Based Composites," *Soft Robotics*, vol. 7, no. 6, pp. 724–735, 12 2020.

[28] D. S. Shah, E. J. Yang, M. C. Yuen, E. C. Huang, and R. Kramer-Bottiglio, "Jamming Skins that Control System Rigidity from the Surface," *Advanced Functional Materials*, vol. 31, no. 1, 1 2021.

[29] R. Baines, S. Freeman, F. Fish, and R. Kramer-Bottiglio, "Variable stiffness morphing limb for amphibious legged robots inspired by chelonian environmental adaptations," *Bioinspiration and Biomimetics*, vol. 15, no. 2, 2020.

[30] B. Aktaş, Y. S. Narang, N. Vasios, K. Bertoldi, and R. D. Howe, "A Modeling Framework for Jamming Structures," *Advanced Functional Materials*, vol. 31, no. 16, 4 2021.

[31] L. Arleo, G. Bondì, S. Albini, M. Maselli, and M. Cianchetti, "Design methodology for the development of variable stiffness devices based on layer jamming transition," *Engineering Research Express*, vol. 3, no. 3, 9 2021.

[32] T. Atakuru, G. Züngör, and E. Samur, "Layer Jamming of Magnetorheological Elastomers for Variable Stiffness in Soft Robots," *Experimental Mechanics*, vol. 64, no. 3, pp. 393–404, 4 2024.

[33] I. Choi, N. Corson, L. Peiros, E. W. Hawkes, S. Keller, and S. Follmer, "A Soft, Controllable, High Force Density Linear Brake Utilizing Layer Jamming," *IEEE Robotics and Automation Letters*, vol. 3, no. 1, pp. 450–457, 1 2018.

[34] A. Rendos, S. Woodman, K. McDonald, T. Ranzani, and K. A. Brown, "Shear thickening prevents slip in magnetorheological fluids," *Smart Materials and Structures*, vol. 29, no. 7, 7 2020.

[35] M. C. Yuen, R. A. Bilodeau, and R. K. Kramer, "Active Variable Stiffness Fibers for Multifunctional Robotic Fabrics," *IEEE Robotics and Automation Letters*, vol. 1, no. 2, pp. 708–715, 7 2016.

[36] K. J. McDonald, L. Kinnicutt, A. M. Moran, and T. Ranzani, "Modulation of Magnetorheological Fluid Flow in Soft Robots Using Electropermanent Magnets," *IEEE Robotics and Automation Letters*, vol. 7, no. 2, pp. 3914–3921, 4 2022.

[37] A. M. Moran, V. T. Vo, K. J. McDonald, P. Sultania, E. Langenbrunner, J. H. V. Chong, A. Naik, L. Kinnicutt, J. Li, and T. Ranzani, "An electropermanent magnet valve for the onboard control of multi-degree of freedom pneumatic soft robots," *Communications Engineering*, vol. 3, no. 1, p. 117, 8 2024.

[38] A. N. Knaian, "Electropermanent Magnetic Connectors and Actuators: Devices and Their Application in Programmable Matter," Ph.D. dissertation, Massachusetts Institute of Technology, 7 2010.